

sider optoelectronic switches made of semi-insulating GaAs with the following parameters: n (refractive index) = 3.6, $(\mu_n + \mu_p)$ (sum of electron and hole mobilities) = $2000 \text{ cm}^2 \text{ V}^{-1} \text{ s}^{-1}$, l (the gap between electrodes) = $3 \mu\text{m}$, $\hbar v$ (incident photon energy) = 1.5 eV and the conductance across the gap is $G = 1 \times 10^{-2} \Omega^{-1} / \text{pJ}$. To switch the output of a polarisation-bistable laser within 1 ns, the current pulse needs to be 40 mA or 2 V across 50Ω .¹ Such voltage can be delivered by the circuit with two optoelectronic switches connected in series shown in Fig. 2a, using 20 V DC bias and 2 pJ energy of the semiconductor laser pulse.

In conclusion, we have demonstrated the operation of a clocked optical S-R flip-flop based on polarisation-bistable semiconductor lasers with very simple circuitry. Other types of optical flip-flops can be constructed with similar schemes.

J. M. LIU
Y. C. CHEN

28th January 1985

GTE Laboratories Incorporated
40 Sylvan Road
Waltham, MA 02254, USA

References

- CHEN, Y. C., and LIU, J. M.: 'Polarization bistability in semiconductor lasers', *Appl. Phys. Lett.*, 1985, **46**, pp. 16-18
- CHEN, Y. C., and LIU, J. M.: 'Temperature dependent polarization behavior in semiconductor lasers', *ibid.*, 1984, **45**, pp. 731-733
- LEONBERGER, F., and MOULTON, P. F.: 'High-speed InP optoelectronic switch', *ibid.*, 1979, **35**, pp. 712-714
- GÖBEL, E. O., VEITH, G., KUHL, J., HABERMEIER, H. U., LÜBKE, K., and PERGER, A.: 'Direct gain modulation of a semiconductor laser by GaAs picosecond optoelectronic switch', *ibid.*, 1983, **42**, pp. 25-27
- HARDER, CH., LAU, K. Y., and YARIV, A.: 'Bistability and pulsation in semiconductor lasers with inhomogeneous current injection', *IEEE J. Quantum Electron.*, 1982, **QE-18**, pp. 1351-1360
- JOHNSON, A. M., and AUSTON, D. H.: 'Microwave switching by picosecond photoconductivity', *ibid.*, 1975, **QE-11**, pp. 283-287

SHUNT-INDUCTANCE-COUPLED WAVEGUIDE FILTERS WITH EXPANDED SECOND STOPBAND

Indexing terms: Filters, Microwave filters

A computer-aided design is described for inductive iris and inductive double-strip coupled filters with increased-width resonator sections. The theory includes both the higher-order-mode interaction of all discontinuities and the finite thickness of the irises and inserts. The step-wall discontinuity effect is included in the optimisation process as an additional design parameter. Design examples for midband frequencies of about 11 and 16 GHz are given; the corresponding stopband attenuation is higher than 50 dB, or 40 dB, up to 18.5 GHz, or 24.5 GHz, respectively.

Introduction: Common rectangular waveguide bandpass filters coupled by inductive irises or E -plane integrated metal strips,¹⁻⁵ are composed of halfwave resonator sections equal in width to the feeding waveguide. Owing to the nonlinear relation between guide wavelength and frequency, however, for this type of filter, high attenuation requirements over a broad second stopband are often difficult to meet. To alleviate the problem, the cutoff frequency of the fundamental mode within the filter resonators may be suitably reduced by increasing the waveguide width in question. Moreover, the inductive junction effect of the step-wall discontinuity may be advantageously utilised as an additional design parameter for shunt-inductance coupled filters.

In this letter, therefore, inductive iris and inductive strip coupled resonator filters within an increased-width waveguide (Fig. 1) are investigated. As in References 3-5, the design of optimised filters is based on a rigorous field expansion technique into incident and scattered waves at all discontinuities. This allows direct inclusion of higher-order mode coupling,

finite strip thickness and the step-wall discontinuity effects in the optimisation process.

Theory and design: The electromagnetic fields of each sub-region at the corresponding discontinuities are derived from the x -component of the magnetic Hertzian vector,³⁻⁵ which is

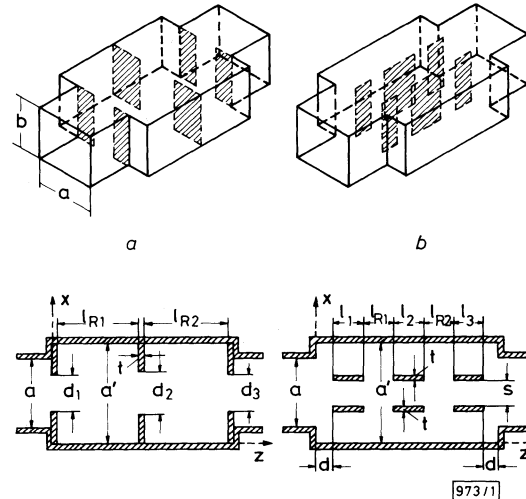


Fig. 1 Shunt-inductance coupled filters with increased-width resonators

- a Inductive iris type
b Inductive double-strip type

assumed to be a sum of the eigenmodes satisfying the wave equation and the boundary conditions at the metallic surfaces:

$$\Pi_{hx} = \sum_{m=1}^M A_m^{\pm} T_m \sin \left[\frac{m\pi}{p} f \right] e^{\mp jk_{zm}z} \quad (1)$$

where M is the number of eigenmodes considered, T_m is the normalisation factor so that the power carried by a given wave is 1 W for a wave amplitude of $1/\sqrt{W}$,³⁻⁵ p is the cross-section dimension (cf. References 3-5) of the subregions at the corresponding discontinuity considered, f is the variable in the x -direction (cf. References 3-5) of the subregion at the corresponding discontinuity considered, and $k_{zm}^2 = k^2 - (m\pi/p)^2$, $k^2 = \omega^2 \mu \epsilon$.

By matching the field components at the corresponding interfaces, the coefficients A_m^{\pm} in eqn. 1 are determined after multiplication with the appropriate orthogonal function (cf. References 3-5). This yields the scattering matrix at the step discontinuity considered. The scattering matrix of the total filter is then calculated by directly combining the single scattering matrices, as in Reference 3. This procedure preserves numerical accuracy, since the direct combination of scattering matrix parameters contains exponential functions with only negative argument.

The computer-aided design is carried out by an optimising program⁵ applying the evolution strategy method which varies the input parameters until the desired values of the insertion loss and of the stopband attenuation, for given bandwidths, are obtained. For additional given input and output waveguide housing dimensions a , b , thicknesses t of the irises or metal strips, respectively, spacing s of the double insert and number of resonators, the parameters to be optimised are the iris apertures d_i , or lengths l_i , of the double insert strips, respectively, the lengths l_{Ri} of the resonators, width a' of the increased width section, and distance d to the step discontinuity (for the double metal insert filter). For computer optimisation, the expansion into 15 eigenmodes at each discontinuity has turned out to be sufficient. The final design data are checked up by 35 eigenmodes.

Results: A five resonator Ku-band filter is chosen for the design example for the inductive irises coupled filter type (Fig. 1a). For comparison, Fig. 2 shows the calculated insertion loss $1/|S_{21}|$ in decibels for the usual iris filter (broken line), for the iris filter within a reduced-width waveguide (dash-dotted line), and for the iris filter within an increased-width waveguide (solid line). The curves demonstrate the better stopband attenuation behaviour of the increased-width filter.

For the inductive strip coupled filter type, the double insert is preferred (Fig. 1b), which, compared with its single insert counterpart, has the advantage that the distance between the strips and the waveguide sidewalls may be suitably chosen to maintain the evanescent field character along the strips over a

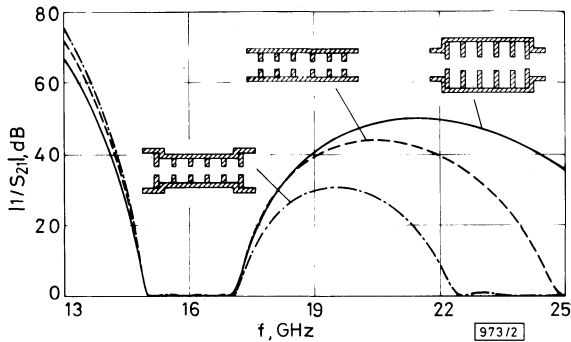


Fig. 2 Insertion loss for an iris-type filter (Fig. 1a) with five resonators

$a = 15.789$ mm, $b = 7.899$ mm; iris thickness $t = 0.19$ mm
 - - - - resonator section width $a' = a$, filter data (cf. Fig. 1a):
 $d_1 = d_6 = 7.112$ mm, $d_2 = d_5 = 5.310$ mm, $d_3 = d_4 = 4.798$ mm,
 $l_{R1} = l_{R5} = 9.357$ mm, $l_{R2} = l_{R4} = 10.119$ mm, $l_{R3} = 10.262$ mm
 - · - · - reduced-width resonator section
 $a' = 12.638$ mm, $d_1 = d_6 = 7.712$ mm, $d_2 = d_5 = 6.022$ mm, $d_3 =$
 $d_4 = 5.440$ mm, $l_{R1} = l_{R5} = 10.361$ mm, $l_{R2} = l_{R4} = 11.493$ mm,
 $l_{R3} = 11.892$ mm
 ——— increased-width resonator section
 $a' = 20.538$ mm, $d_1 = d_6 = 7.388$ mm, $d_2 = d_5 = 5.266$ mm, $d_3 =$
 $d_4 = 4.634$ mm, $l_{R1} = l_{R5} = 8.491$ mm, $l_{R2} = l_{R4} = 9.377$ mm,
 $l_{R3} = 8.49$ mm

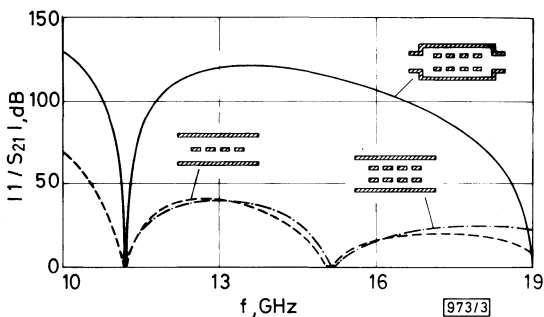


Fig. 3 Insertion loss for a double-insert-type filter (Fig. 1b) with three resonators

$a = 15.799$ mm, $b = 7.899$ mm
 - - - - resonator section width $a' = a$, single-insert type, insert
 thickness $t = 0.19$ mm, filter data (cf. Fig. 1b): $l_1 = l_4 = 0.03$ mm,
 $l_2 = l_3 = 4.596$ mm, $l_{R1} = l_{R3} = 19.201$ mm, $l_{R2} = 21.534$ mm
 - · - · - resonator section width $a' = a$, double-insert type,
 $t = 0.19$ mm, $s = 5.0$ mm, $l_1 = l_4 = 0.02$ mm, $l_2 = l_3 = 1.656$ mm,
 $l_{R1} = l_{R3} = 19.996$ mm, $l_{R2} = 22.832$ mm
 ——— increased-width resonator section
 $a' = 25.2$ mm, double-insert type, $t = 3$ mm, $s = 4.2$ mm,
 $d = 14.48$ mm, $l_1 = l_4 = 1.279$ mm, $l_2 = l_3 = 9.356$ mm, $l_{R1} =$
 $l_{R3} = 14.516$ mm, $l_{R2} = 14.535$ mm

wide frequency band.⁴ Fig. 3 shows the calculated insertion loss for a three-resonator single metal insert filter (broken line), a double metal insert filter (dash-dotted line), and for a double metal insert filter within an increased-width waveguide (solid line). The advantage of the increased-width filter type is evident.

Conclusion: Improvement of the stopband behaviour of shunt inductance coupled waveguide filters is possible by increasing the waveguide width within the resonator sections. The reduction of the cutoff frequency of the resonators increases the frequency spacing between the first and the second pass-band. Moreover, the inductive junction effect of the step discontinuity may be utilised as an additional design parameter to be optimised. Since the computer-aided design is based on field expansion into eigenmodes, higher-order mode coupling effects at all discontinuities and the finite thickness of the metal irises, and inserts, respectively, are taken into account. Examples for iris and double insert coupled resonator filters

with an increased-width waveguide section demonstrate the excellent stopband behaviour of this class of filters.

F. ARNDT
 J. BORNEMANN
 C. PIONTEK
 H. SCHÜLER

4th February 1985

Microwave Department
 University of Bremen
 Kufsteiner Str., NW 1, D-2800 Bremen 33, W. Germany

References

- MATTHAEI, G. L., YOUNG, L., and JONES, E. M. T.: 'Microwave filters, impedance-matching networks, and coupling structures' (McGraw-Hill, New York, 1964), pp. 450-459, 540
- KONISHI, Y., and UENAKADA, K.: 'The design of a bandpass filter with inductive strip—Planar circuit mounted in waveguide', *IEEE Trans.*, 1974, **MTT-22**, pp. 869-873
- PATZELT, H., and ARNDT, F.: 'Double-plane steps in rectangular waveguides and their application for transformers, irises and filters', *ibid.*, 1982, **MTT-30**, pp. 155-163
- ARNDT, F., BORNEMANN, J., VAHLDIECK, R., and GRAUERHOLZ, D.: 'E-plane integrated circuit filters with improved stopband attenuation', *ibid.*, 1984, **MTT-32**, pp. 1391-1394
- VAHLDIECK, R., BORNEMANN, J., ARNDT, F., and GRAUERHOLZ, D.: 'W-band low-insertion loss E-plane filter', *ibid.*, 1984, **MTT-32**

20 GHz ACTIVE MODE-LOCKING OF A 1.55 μ m InGaAsP LASER

Indexing terms: Lasers and laser applications, Semiconductor lasers

Active mode-locking of a 1.55 μ m wavelength InGaAsP laser at repetition rates up to 20 GHz is reported. The pulsewidth is 5 ps at 20 GHz, with a peak pulse power of 18 mW coupled into a single-mode output fibre.

Short-duration mode-locked optical pulses at multigigahertz repetition rates will find application in future communication and signal-processing systems. The highest mode-locked repetition rates reported to date have been 10 GHz in InGaAsP lasers at 1.3 μ m wavelength¹ and 18 GHz in AlGaAs lasers.² The main limitations on the maximum observed repetition rate in Reference 1 were the relatively large pulsewidth (30 ps) and the finite bandwidth of the photodetector and associated instrumentation. We recently demonstrated† a decrease in pulsewidth (to 5 ps) using an actively mode-locked 1.55 μ m InGaAsP laser in a new single-mode-fibre composite-cavity resonator structure. The present letter reports mode-locking in this structure at repetition rates up to 20 GHz. This is the highest repetition rate so far reported in a mode-locked semiconductor laser.

The InGaAsP laser-fibre composite cavity† is illustrated in Fig. 1. It uses a 1.55 μ m three-channel buried-crescent (TCBC) laser with low parasitic capacitance and high modulation bandwidth.³ One facet of the laser chip is coated with a high-reflectivity ($R_1 > 0.9$) multilayer dielectric mirror. The other facet is coated with a single-layer antireflection (AR) coating, with a residual reflectivity of $R_2 \sim 2 \times 10^{-4}$. The AR-coated facet is optically coupled to a 5 cm single-mode-fibre resonator with a microlens at one end. The other end of the resonator is coated with a partially reflecting multilayer dielectric mirror with a reflectivity of $R_3 = 0.6$. The output from the composite cavity is coupled through this mirror into a second single-mode fibre, which is terminated at a biconical output connector. The laser chip is mounted in a broadband 50 Ω microwave test fixture, and the DC and RF components of the drive signal are combined in a bias tee.

In our first series of experiments using this structure† the

† EISENSTEIN, G., TUCKER, R. S., KOROTKY, S. K., KOREN, U., STULZ, L. W., JOBSON, R. M., VESELKA, J. J., and HALL, K. L.: 'InGaAsP 1.55 μ m mode-locked laser with a single-mode-fibre output', submitted to *Electron. Lett.*